Experimental study on load sharing characteristics of long-short CFG pile composite foundation adjacent to rigid retaining wall rotating about its base

Bantayehu Uba Uge*, ** and Yuan-Cheng Guo*

*School of Civil Engineering, Zhengzhou University, Zhengzhou 450001, China

**School of Civil Engineering, Hawassa University, Hawassa, Ethiopia

* Corresponding Author: guoyuancheng@163.com

Submitted: 28-12-2020

Revised: 02-10-2021

Accepted: 12-10-2021

ABSTRACT

Practicing geoengineers and researchers generally consider the load sharing behavior in multi-type pile composite foundation as an important design aspect. On the other hand, due to urbanization, such foundation system in cities will inevitably appear next to supported excavation. This paper discusses the result from relatively large-scale indoor experiment conducted to investigate the load sharing behavior of loaded long-short CFG pile composite foundation behind a neighboring rigid retaining wall undergoing rotation around the bottom. It was found that with progression of wall movement, the hidden load from soil displacement was borne by the piles with marked reduction in soil load sharing. At the end of wall rotation, the percentage of long piles' head load increment needed to arrive at a new static equilibrium was about 12.57~32.22% while the end bearing increased by more than 97%. The consequences on the short piles, however, were manifested with an increasing pile head (13.42%) and toe (28.9%) load for the pile far from the wall whereas the closest one experienced a certain increment up to 15×10^{-4}rad wall rotation and finally the head load and end bearing decreased to 8.28% and 12.63%, respectively. The 3D numerical back analysis conducted using FE software ABAQUS yielded the pile – soil stress ratio lower than the value obtained from the experiment but provided great insight into pile settlement characteristics during wall rotation.

Keywords: Rigid retaining structure, Disconnected piled raft, Composite foundation, Load sharing ratio, Cushion

INTRODUCTION

The load sharing characteristics is a key factor to describe the mechanical behavior and load – carrying mechanism of Cement-Fly ash- Gravel (CFG) piled raft composite foundation. It reflects the coordination ability of the pile and shallow weak soil layer of the composite foundation in transferring applied load from superstructure to the ground. Since the invention of this novel column-type ground improvement technology, enormous analytical, experimental and numerical studies have been reported to comprehend its mechanical characteristics and application areas (Cai, 2014; Guo et al., 2011; Lu et al., 2015; Shen et al., 2017; Shen and Wang, 2016; Zhang et al., 2018). Uge and Guo (2020) have recently given a succinct overview on the remarkable developments and its implementation in different infrastructure projects.

At present, literature is rich with information regarding pile – soil stress ratio, capability of cushion to evenly transmit upcoming vertical load to pile head and soil, relative pile – soil displacement and its associated negative skin friction (NSF) development on the upper 15 ~ 50% of the length of pile, bearing and settlement characteristics, and utilization of different kinds of pile types. Even though the NSF on the upper pile section is one of the common features in disconnected piled rafts (Jiang and Liu, 2018; Miao et al., 2018; Saeedi Azizkandi et al., 2019; Wu et al., 2016; Zhu, 2017), it is considered as unfavorably imposed action in traditional pile design. Nonetheless, equilibrium is achieved with necessary pile/soil relative movement for positive shaft friction (PSF) and/or sufficient pile settlement to mobilize tip resistance by the so called "natural self-balancing process" (Tan and

Fellenius, 2016).

Just like all the other foundation system in real project, long-short pile composite foundations experience both vertical and lateral loadings (Poulos, 2007). However, compared to vertical bearing characteristics, studies on lateral bearing behavior of are still limited, probably because of the complex soil structure interaction. According to the review work of Uba Uge and Guo (2020), the risk control practice of disconnected piled rafts adjacent to excavation work requires a holistic risk management plan to capture the complex soil – structure interaction thereof. The overall safety of existing buildings and historic centers is the most concerning issue when excavation is carried out nearby; particularly, as developments in condensed urban dwellings call for a spate of excavations for new high-rise buildings and underground space utilization (Abd Elrehim and Abd Ellaah, 2016; Korff et al., 2016; Liang et al., 2019; Mu et al., 2020; Shakeel and Ng, 2018). On the face of it, more and more excavation work due to urbanization are becoming evident around existing CFG composite foundations that would affect their load distribution mechanism.

Unless otherwise the retaining wall yielding is kept under a permissible range, the resulting soil movement would influence the performance of disconnected piled raft composite foundation system. However, in recent years, many researchers have highly been drawn towards evolution and distribution of earth pressure on retaining wall neighboring CFG pile composite foundation (Li et al., 2012; L. Li et al., 2019; M. Li et al., 2019b). According to the numerical analysis of Ji and Ge (2013), the static geotechnical model test performed by Wei (2018) and centrifuge experimental study conducted by Li et al. (2018), the lateral active earth pressure on the retaining wall is smaller than the value predicted from the conventional methods due to the reduction in lateral displacement of the treated backfill as compared to the natural intact ground.

Scholars such as Wang and Yang (2013) and Fu and Li (2021) have conducted model test and centrifuge tests, respectively, to observe the phenomenon of load sharing mechanism in CFG pile composite ground during the process of nearby excavation. M. Li et al.(a) (2019) have also experimentally studied the load distribution of rigid – pile composite foundation under the influence of retaining wall rotation. The results from these studies demonstrated that there is significant variation in axial load along the pile length and pile-soil stress ratio at different stages of the excavation, with the final construction step producing substantial change. Each of those studies has been conducted on piles of equal length. However, when different types/lengths of piles are comprised in the system, apprehending the soil-structure interaction mechanism becomes relatively complicated. The current study aims to discuss the load sharing mechanism in rigid long-short piled raft composite foundation, based on an indoor model experiment with rigid wall rotating about its base. Observations on the influences of wall rotation induced soil movement on the pile head load, end bearing capacity and pile/soil load sharing characteristics are presented.

EXPERIMENTAL DETAILS

Model enclosure and data acquisition system

Fig. ***1*** shows the schematic representation of the 1.6m×1.6m×2.5m model box test setup developed by the Research Institute of Geotechnical Engineering at Zhengzhou University, China, which was sufficient to ignore boundary effects for the size of the model piled raft. The front side of the wall was specially designed to enable rotation/translation movement of wall manually with symmetrically placed displacement control screw rods, pivot and slideway at its lower end. The rear wall involved ten dismountable small rectangular plates to control the wall height during soil filling and unloading at any desired moment. The side walls, that were made of 5mm thick steel plate and stiffened by square section steel frame, were remained stationary. Rigid reaction frame was placed external to the sidewalls.

The model raft was made of plain carbon structural steel plate of dimension 600mm×600mm×50mm and satisfied the square raft-soil stiffness definition given by (Horikoshi and Randolph, 1997). Standard sand and fine Zhengzhou city river sand were used respectively as cushion and analogous foundation soil to meet the test requirements in Chinese technical specification GB/T 50783-2012 (2012). The cushion layer had a thickness of 50mm. The maximum and minimum dry density of the fine sand was 1.795g/cm3 and 1.592g/cm3, respectively.

Closed ended aluminum hollow pipe piles of length 1000mm and 2100mm were used according to similarity law as short and long piles respectively, each having an outer diameter of 100mm and thickness 3mm. The scaling effect was taken into account with the length similarity ratio (λ_L) of 3. The pile shaft surface was made rough through knurling that resulted in 27.3° interface frictional angle. The strain gauges attached at 200mm intervals on the inner smooth surface of piles marked couplets opposite to each other, symmetrically, at four points

on the same section of the pile periphery. Pressure cells were attached at the ends of each pile to measure the head and toe loads.

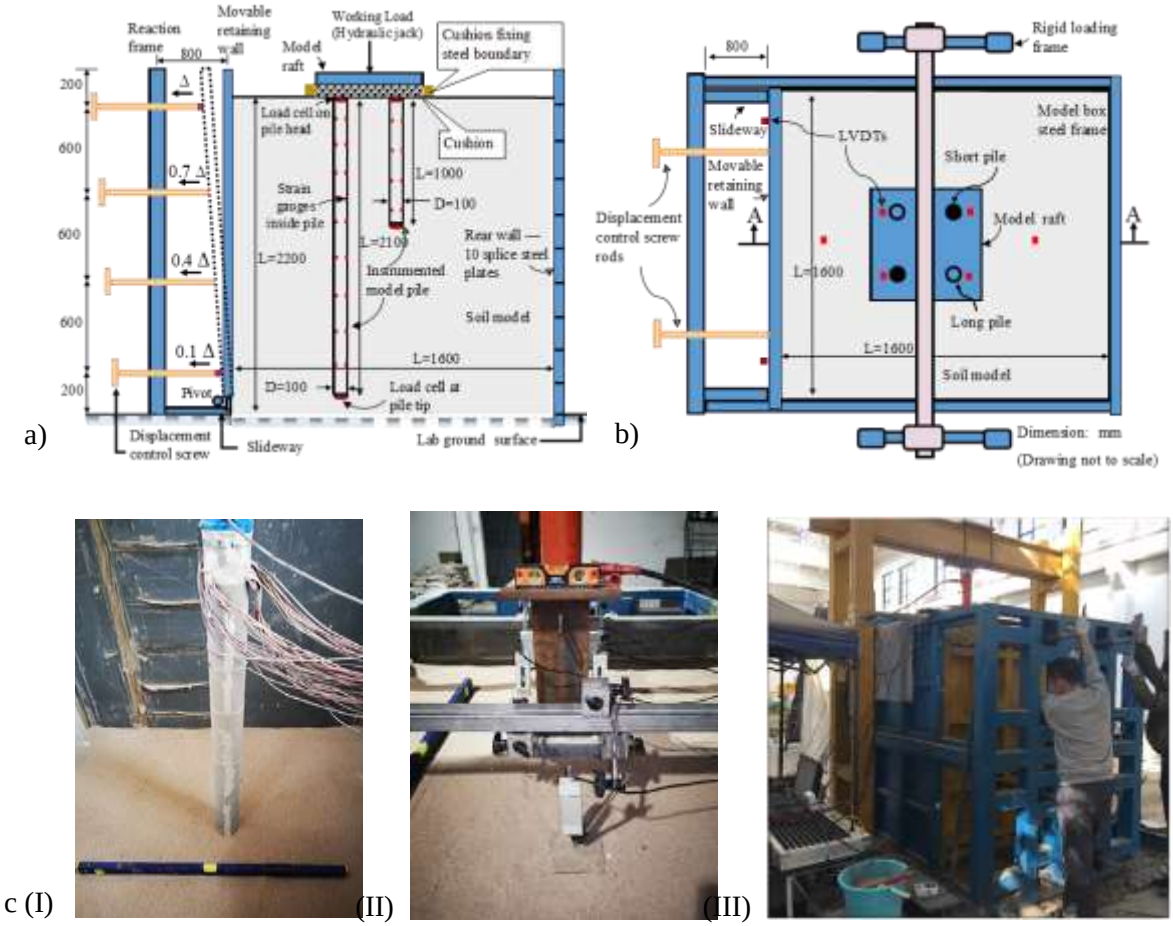

Fig. 1. Schematic view of the test model set-up: a) sectional view (section A-A), b) plan view, c) photographs taken during (I) instrumented pile embedment, (II) raft & hydraulic jack placement on top of the cushion, and (III) wall rotation

Hydraulic jack mounted with load cell was used to apply the vertical working load. The load borne by the soil between piles were measured by earth pressure cells placed on the sand surface beneath the cushion. Raft surface settlement and wall rotation were measured by LVDT displacement sensors. Prior to experiment, each earth pressure and load sensor were verified for repeatability and stress hysteresis effect through indoor calibration test.

Testing procedure

The testing procedure consisted two major steps: the first step where the vertical foundation load was applied and the last in which front wall rotation under the applied load was made. The sand bed was prepared by pouring and tamping technique with the sand being freely dropped form the height of the model box by a conveyor belt. The thickness of each layer was planned to be 300mm at 45% degree of compaction. The average density value of the fill was 1.621g/cm^3. Once the fill was made to the level of prescribed pile toe, the pile was positioned vertically and the next layer was continued to the final surface. At the top final levelled sand surface, the cushion layer was placed bounded by steel frame. Then, the hydraulic jack was mounted on the loading plate stationed on top of the cushion. Prior to the loading process, the model ground was kept still for a week in order to balance the stress state of the soil.

Chinese codes (JGJ340-2015, 2015), (JGJ106-2014, 2014) and (JGJ 79—2012, 2012) were followed in the first step. The codes recommend to divide the presumed loading into 8~12 levels; and when the settlement for each level of loading is less than 0.1mm for an hour and more, the next to be applied. Accordingly, the loading was divided into 10 levels and the test was terminated when the settlement reached 1% of the loading plate breadth. Testes for both single short pile composite foundation and single long pile composite foundation were also conducted with a foundation plate of plan dimension 300mm×300mm but are presented here with limited emphasis

for the sake of space brevity.

In the second stage, the top of front wall was displaced laterally by an amount =10mm (0.5% of wall height) in 10 states as per existing in-house research works on rotation amount required to attain the active limit state (M. Li et al., 2019b; Wei, 2018). In doing so, the displacement of screw rods was manually controlled to simultaneously obtain 1mm at each stage according to the calibration of screw rode rotation to yield the same. After the data of each stage was stable, the next rotation was carried out. Since settlement had occurred as wall rotation advanced, the applied load on the foundation had consequently been sustained manually to maintain the hydraulic jack pressure unchanged throughout the process.

RESULTS AND DISCUSSION

Analysis of test result during loading process

The load settlement curve of single short pile (1.0m long), single long pile (2.1m long), and four long-short pile (of length 2.1m, and 1.0m) composite foundation is depicted in ***Fig. 2***. (a). ***Fig. 2***. (b) shows the variation of pile head load of four long - short pile composite foundation during loading step as a function of the overall settlement (*S*) relative to raft width (*Br*). For comparison, the results for single pile composite foundation have also been depicted. In the current experiment, the settlement of soil between piles has not been measured.

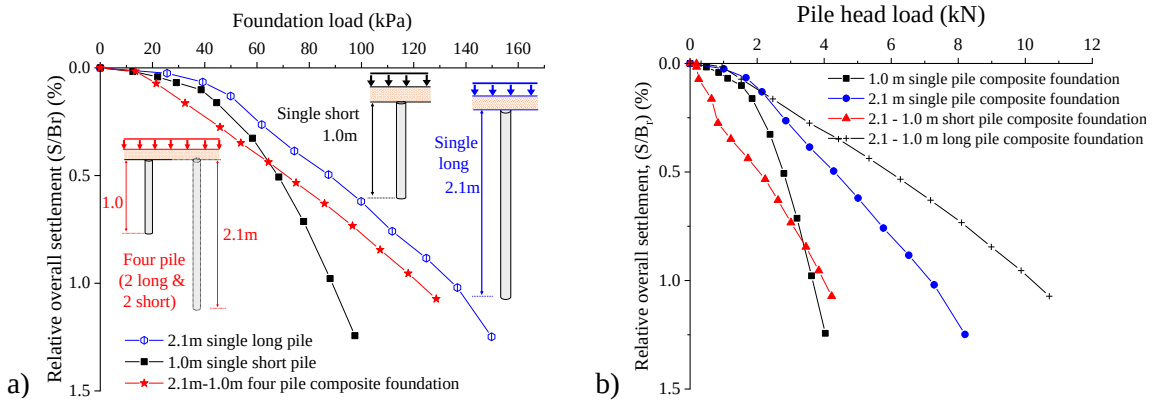

Fig. 2. Load carrying behavior during first step (a) imposed load - settlement curve (b) pile head load with respect to overall composite foundation settlement

As can be seen from ***Fig. 2***, the characteristic value of bearing capacity at the settlement of 1% of *Br* were 87kPa, 127kPa, and 117kPa, respectively for single short, single long and four long-short pile composite foundation. Only the single short pile composite foundation has demonstrated a clear inflection point, which was in the range between 40 ~ 50kPa. Moreover, as reported by Hou (2020), for a given foundation stress, the overall stiffness of single pile composite foundation was found to be higher than that of four long-short pile composite foundation. Under the group action of the piles, the difference of stress state between piles could have attributed to the decrease in overall stiffness of the four piles composite foundation. The soil between piles in the four piles composite foundation had borne greater load as compared to that in the single pile composite foundation for the same applied load level. From the pattern of the load borne by the piles in the long-short pile composite foundation, it is evident that stresses on top of long piles were much higher than that on short piles.

The variation of pile – soil stress ratio illustrated in ***Fig. 3***. (a) was calculated as the ratio of the stress on top of the pile to that on the surface of the soil. The gap between each curve indicates that the rate at which the stress increased on the long pile head was higher than that of the short pile as the imposed load increased, which could easily be observed from ***Fig. 2*** as well. Some scholars have also revealed the same, in which the load sharing ratio of long pile increases gradually while sharply falls for short pile (Qian and Zhang, 2014). As can be observed from the illustration in ***Fig. 3.*** (b) about the pile and soil load sharing variation with loading, the load proportion taken by piles increased and that borne by the soil gradually decreased as the applied load was increased. Noticeably, transfer of stress to soil between piles at lower loading was higher; and rapidly dropped as the cushion played its role to adjust the load transmission to the relatively stiffer material. In the initial loading stage, majority of the foundation stress was borne by the soil. For the vertical loading beyond 60kPa, the rate of increase in pile head load and the decrease in stress borne by the soil between piles were continued to occur slowly due to progressive mobilization

of pile resistance and later followed approximately a steady pattern.

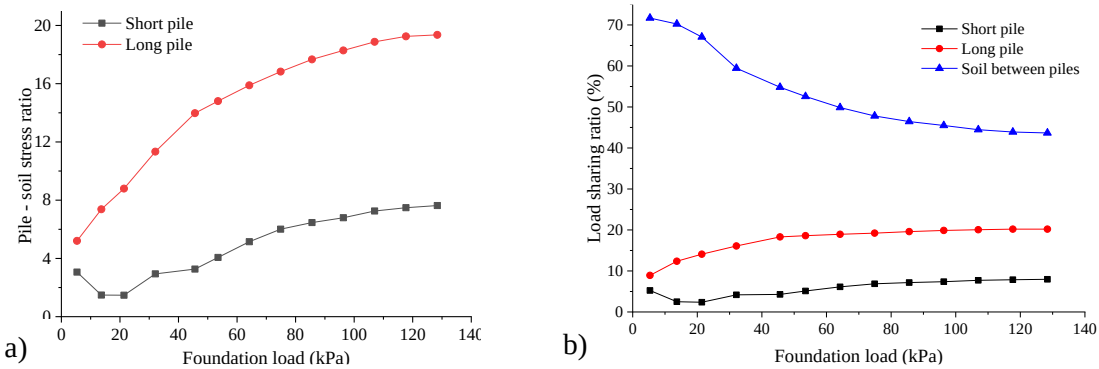

Fig. 3. (a) Pile - soil stress ratio and (b) load sharing proportion of long-short pile composite foundation during loading process

Analysis of test results during wall rotation about its base

In order to understand how soil displacement affects the load sharing behavior of long-short pile composite foundation, the front retaining wall movement was conducted at the end of the loading process. Once the retaining structure started rotating about its base, displacement of the soil behind the wall triggered settlement of the soil between piles. As a result, the stress borne by the soil between piles continued to decrease and accordingly, the stress on the head of each pile increased to sustain the balance. Similarly, with the increase of wall rotation, the stress of the pile toe also increased except for the front short pile which showed slightly declining pattern after wall rotation reached a value of 15×10^{-4}rad. These phenomena can be observed from ***Fig. 4*** that at the end of wall rotation, the front and rear long piles had to bear an additional pile head load of 12.56% and 32.22%, respectively. When it comes to pile end-bearing, the percentage increment had reached almost 100% (97.35% and 98.97% respectively for the front and rear long pile). However, for the short piles, both the head and tip bearing were found to decrease (8.28% and 12.63% respectively) for the front pile while increased for the rear one (13.42% and 28.9% respectively).

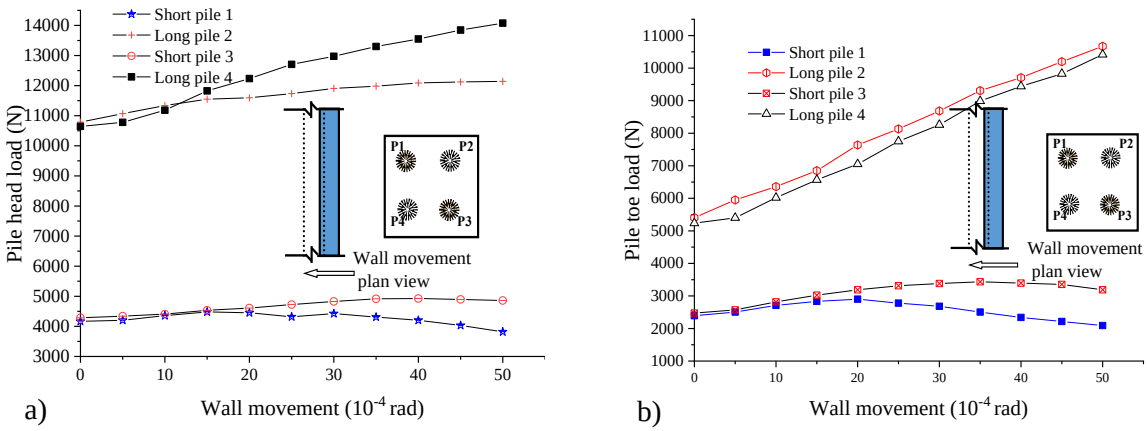

Fig. 4. Variation of pile (a) head load and (b) tip resistance during wall rotation about its base

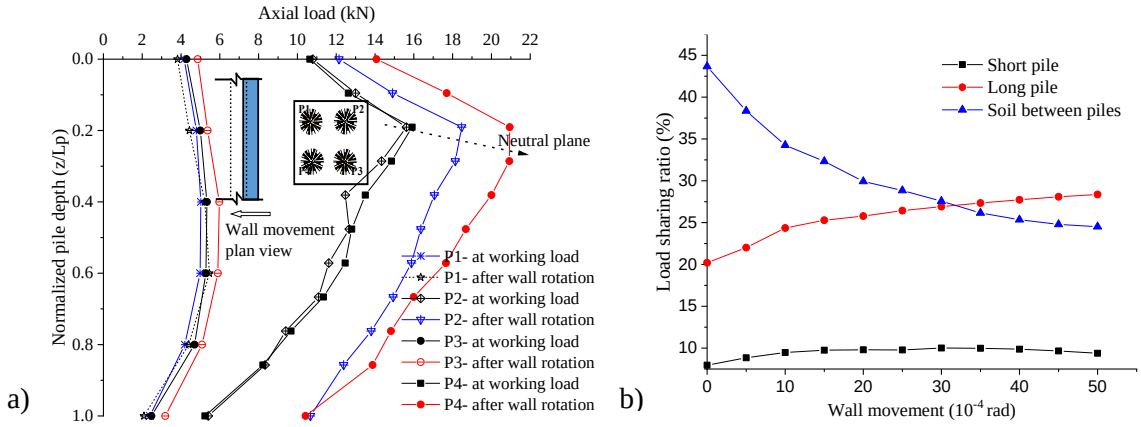

Fig. 5. Variation of (a) axial force with depth and (b) pile and soil load sharing during wall rotation about its base

The axial load change along the pile length at the end of wall rotation are presented in ***Fig. 5.*** (a) with normalized depth in comparison with its distribution before rotation begun. Due to the action of the ground displacement, NSF is mobilized in the upper pile section and hence increase in axial force distributed in this section of the pile body. After a certain depth between 0.24 ~ 0.6 times the pile length, where the NSF turns into PSF, the normal force distribution in the pile body begins to decrease. As expected, the soil displacement induced pile dragged down and the applied foundation load were equilibrated by bearing additional pile head load and substantial pile tip settlement to develop extra end – resistance. It can also be observed that the load transfer mechanism involves both downward and upward load transfer mechanism; with the neutral point moving downward as the wall movement continues.

The load sharing proportion during wall rotation is presented in ***Fig. 5***.(b). It is well known that wall movement induced soil displacement field attenuates as the distance from the wall increases. Consequently, the additional stress increment at the top and toe of the piles were different, where the front long pile had taken the load at a relatively higher rate than the long pile far from the wall. To this end, the load sharing ratio of soil between piles decreased proportionally. What is interesting is that the applied load, which was manually kept as constant as possible in the process of wall rotation, led to an increase in the pile-soil stress ratio as well. An important notice from this is the redistribution of the applied load within the group. This was because of the reduction in bearing capacity of the soil between piles due to the soil displacement. Experimental results reported by M. Li et al. (a) (2019) on four piles with 2.1m equal length composite foundation agrees to this observation where the front piles that were close to the wall have had a higher stress increment in comparison to the rear piles. The difference is that for four long-short piles in the current experiment, the front long pile had almost close increment with the rear long pile but with significant difference on the load received by the short piles. Consequently, the additional load in the short pile was mainly transferred to its tip bearing resistance and some shifted to be borne by the long piles.

NUMERICAL BACK ANALYSIS

To enhance understanding on the pattern of the response, the experiment was back analyzed using ABAQUS with same plan geometrical dimensions. The depth of model ground was set to be twice the length of long pile. ***Fig. 6*** shows the FE mesh employed for this purpose. It was described by C3D8R element. The boundary was set to prevent out of plane lateral displacement along the sides and constrain both vertical and lateral movement of the base. To reproduce the restraining frame provided to confine the cushion during the experiment, the sides of the cushion part were restrained from lateral movement and so was done to the raft. Mohr-Coulomb (MC) yield criterion was used to model material behavior for geomaterials whereas elastic constitutive relationship was adopted for structural elements. Contacting surfaces were established based on surface-to-surface interaction using penalty friction algorism. Moreover, solid pile was used instead of hollow pile with similar flexibility. After subjecting the whole model to geostatic stress field, distributed vertical load was imposed stage-by-stage on top surface of the raft. Other model parameters are listed in ***Table 1***.

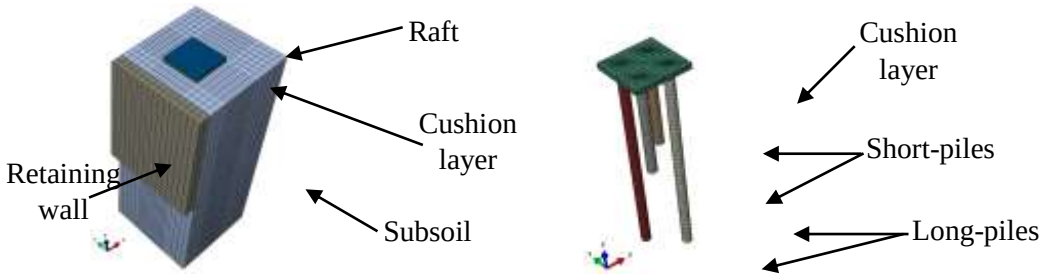

Fig. 6. The 3D and internal view of FE mesh of the composite foundation and retaining wall

Table 1. Material properties used

Property / Material type	Elastic Modulus [MPa]	Poisson's ratio	Density [kg/m^3]	Angle of internal friction [°]	Cohesion [kPa]
Cushion	15.00	0.30	1416	33.90	4.00
Soil	10.50	0.30	1618	33.42	6.48
Pile	8.14×10^3	0.20	2700	–	–
Retaining wall	210×10^3	0.10	7800	–	–
Raft	210×10^3	0.20	7800	–	–

As shown in ***Fig. 7***. (a), the load settlement response curve of four long – short pile obtained from the FE analysis fits almost comparably to experimental result. However, the FEA underestimates the pile load sharing ratio because the stress borne on top surface of the inter-pile soil was higher. The difference might have appeared as a result of the relatively loose state of sand in the upper layer during experiment as compared to the state encountered in the 3D simulation. The load sharing behavior pattern from the current 1 g model test and the FEA can well be taken as a guide to prototype performance; however, more realistic approximations particularly from FEA can be found by incorporating the effect of confining stress increment on soil stiffness with depth (Poulos, 1986; Shi et al., 2019). Moreover, some computational shortcomings would appear because of adopting the MC model, C3D8R element and zero-thickness contact algorithm. Since the stress and strains are computed at the integration points at the middle of C3D8R elements, it was expected that the use of smaller mesh sizes around high stress zones would reduce the limitations associated with the reduced-integration in capturing stress concentrations.

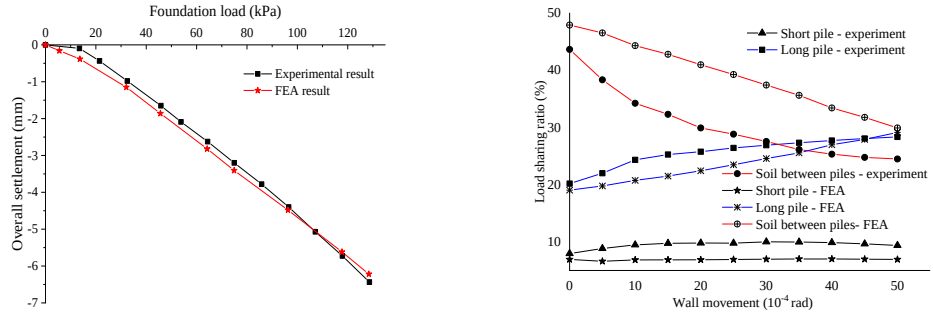

(a) (b)

Fig. 7. Comparison of experimental (a) load settlement curve and (b) load sharing ratio during wall rotation with finite element analysis result

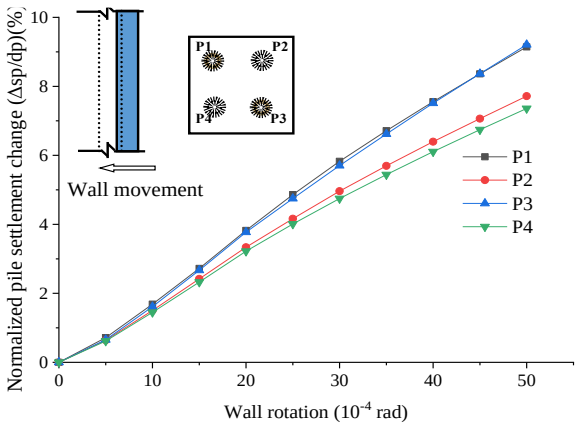

Fig. 8. FE computed additional normalized pile settlement induced during wall rotation about base

Fig. 8 displays change in incremental wall rotation induced pile settlement computed from the FEA. It can be observed that the settlement of short piles is more pronounced during wall rotation with higher rate as compared to long piles. In addition, as the wall rotated, the sliding surface of the soil mass gradually developed (not shown here for space brevity) from top surface to bottom generating larger soil settlement near the wall. This phenomenon reduced the bearing characteristics of soil between front piles so that the end bearing of front short pile became higher in earlier stage to mobilize the additional stresses with increased toe penetration. As the wall rotation continued, the sliding surface further developed to a depth covering large portion of the short pile body. Consequently, the front short pile toe displacement tended to follow the soil displacement vector (flow towards wall) while its head inclined away from the wall with rigid body type tilting. It implies that pile tip location relative to depth of axis of wall rotation probably influences the response of pile to the "drag-load" imposed from soil displacement during wall rotation. This is in agreement with the effect of tip location on load transfer mechanism of floating piles under NSF because of relative pile – soil movement evolving from a surcharge load acting on the surrounding soil (Jeong et al., 2004; Lv et al., 2013). Moreover, due to the considerable portion of the front long pile body within the sliding soil wedge, the mobilized shaft resistance along the length of the pile was transferred to the toe through further settlement to develop more end-bearing resistance. This is also in agreement with the finding by (Soomro et al., 2019) that pile end resistance has to increase in the form of further toe settlement to compensate the reduction in shaft resistance due to excavation induced stress relief.

CONCLUSIONS

From the results, the following findings have been found:

- With the increase of wall rotation about its base, stress received by both the long and short piles have increased while the stress borne by the soil between piles decreased. The overburden load was further redistributed into the head of the piles to remain in quasistatic equilibrium as the soil moves.
- The rate of long pile's head stress increment was higher than that of short piles. Due to larger soil displacement close to the wall, the long pile near the wall experienced larger head stress than the far pile. On the other hand, the pile head stress increment for the rear short pile was larger than that of the front short pile.
- The depth of pile tip relative to axis of wall rotation may affect the response of the pile. The sliding soil mass pronounces the settlement of short piles larger than the long piles. Further pile settlement occurs to mobilize end bearing resistance in order to support the down drag caused by wall rotation induced soil displacement.

ACKNOWLEDGMENT

This research work was funded by Zhengzhou University under a grant from the National Natural Science Foundation of China (51508522).

REFERENCES

Abd Elrehim, M.Z., Abd Ellaah, A.T., 2016. Effects of using Concrete Pre-Supporting Systems with NATM in construction of Underground Stations. J. Eng. Res. 4, 5. https://doi.org/10.7603/s40632-016-0005-3

Cai, J., 2014. Indoor experiment study and mechanism analysis of long-short-pile composite foundation (PhD Dissertation). Taiyuan University of Technology, China.

Fu, Q., Li, L., 2021. Vertical Load Transfer Behavior of Composite Foundation and Its Responses to Adjacent Excavation: Centrifuge Model Test. Geotech. Test. J. 44, 20180237. https://doi.org/10.1520/GTJ20180237

Guo, Y.C., Zhang, S.H., Shi, G., Liu, N., 2011. Optimization Strategy of the Long-Short-Pile Composite Foundation Based on the Settlement Control. Adv. Mater. Res. 243–249, 2429–2434. https://doi.org/10.4028/www.scientific.net/AMR.243-249.2429

Horikoshi, K., Randolph, M.F., 1997. On the definition of raft—soil stiffness ratio for rectangular rafts. Géotechnique 47, 1055–1061. https://doi.org/10.1680/geot.1997.47.5.1055

Hou, S., 2020. Research on force transmission mechanism and design theory of rigid long-short pile composite foundation (PhD Dissertation). Zhengzhou University, China.

Jeong, S., Lee, J., Lee, C.J., 2004. Slip effect at the pile-soil interface on dragload. Comput. Geotech. 31, 115–126. https://doi.org/10.1016/j.compgeo.2004.01.009

Ji, Q.X., Ge, X.S., 2013. The Research on the Influence of the Forms of Foundation on the Behavior of Adjacent Excavation Based on Building Materials. Adv. Mater. Res. 788, 606–610. https://doi.org/10.4028/www.scientific.net/AMR.788.606

Jiang, W., Liu, Y., 2018. Determination of neutral plane depth and pile-soil stress ratio of the rigid pile composite foundation. Rock Soil Mech. 39, 4554–4560. https://doi.org/10.16285/j.rsm.2017.0812

Korff, M., Mair, R.J., Van Tol, F.A.F., 2016. Pile-Soil Interaction and Settlement Effects Induced by Deep Excavations. J. Geotech. Geoenvironmental Eng. 142, 04016034. https://doi.org/10.1061/(ASCE)GT.1943-5606.0001434

Li, L., Huang, J., Han, B., 2018. Centrifugal Investigation of Excavation Adjacent to Existing Composite Foundation. J. Perform. Constr. Facil. 32, 04018044. https://doi.org/10.1061/(ASCE)CF.1943-5509.0001188

Li, L., Huang, J., Ji, X., 2019. Lateral pressures on retaining wall of composite foundation in clayey soils. Chin. J. Geotech. Eng. 41, 89–92. https://doi.org/10.11779/CJGE2019S1023

Li, L., Zhang, H., Xu, B., Wang, Y., 2012. Optimization of excavation supporting structure considering lateral reinforcement effect of CFG composite foundation on soils. Chin. J. Geotech. Eng. 34, 500–506.

Li, M., Qian, Y., Guo, Y., Wei, Y., 2019a. Study on Influence of retaining wall rotation on load distribution of rigid − pile composite foundation. J. Shenyang Jianzhu Univ. Nat. Sci. 35, 655–662.

Li, M., Qian, Y., Guo, Y., Wei, Y., Zhao, S., Cui, X., 2019b. Design of lateral soil pressure model test scheme for adjacent composite foundation. Mech. Eng. 41, 157–163. https://doi.org/10.6052/1000-0879-18-418

Liang, Y.-Y., Liu, N.-W., Yu, F., Gong, X.-N., Chen, Y.-T., 2019. Prediction of Response of Existing Building Piles to Adjacent Deep Excavation in Soft Clay. Adv. Civ. Eng. 2019, 1–11. https://doi.org/10.1155/2019/8914708

Lu, H., Gao, Q., Zhou, B., Wang, D., Liang, M., 2015. Experimental Research on Bearing Capacity of Long-and-short Pile Composite Foundation. Chin. J. Undergr. Space Eng. 11, 56–63.

Lv, Y., Ding, X., Wang, D., 2013. Effects of the tip location on single piles subjected to surcharge and axial loads. Sci. World J. 2013. https://doi.org/10.1155/2013/149706

Miao, L., Wang, F., Lv, W., 2018. A Simplified Calculation Method for Stress Concentration Ratio of Composite Foundation with Rigid Piles. KSCE J. Civ. Eng. https://doi.org/10.1007/s12205-018-1558-5

Mu, L., Chen, W., Huang, M., Lu, Q., 2020. Hybrid Method for Predicting the Response of a Pile-Raft Foundation to Adjacent Braced Excavation. Int. J. Geomech. 20, 04020026. https://doi.org/10.1061/(ASCE)GM.1943-5622.0001627

National standard of the people's republic of China (GB/T 50783-2012), 2012. Technical code for composite foundation. China Planning Press, Beijing, China.

National standard of the people's republic of China (JGJ 79—2012), 2012. Technical code for ground treatment of buildings. China Architecture & Building Press, Beijing, China.

Poulos, H.G., 2007. Ground Movements – A Hidden Source of Loading on Deep Foundations. DFI J. - J. Deep Found. Inst. 1, 37–53. https://doi.org/10.1179/dfi.2007.004

Poulos, H.G., 1986. Pile behaviour - theory and application. Géotechnique 39, 365–415.

Qian, S., Zhang, L., 2014. Study on Bearing Mechanism of Long-short -pile Composite Foundation under Rigid Foundation. Appl. Mech. Mater. 638–640, 570–573. https://doi.org/10.4028/www.scientific.net/AMM.638-640.570

Saeedi Azizkandi, A., Rasouli, H., Baziar, M.H., 2019. Load Sharing and Carrying Mechanism of Piles in Non-connected Pile Rafts Using a Numerical Approach. Int. J. Civ. Eng. 17, 793–808. https://doi.org/10.1007/s40999-018-0356-2

Shakeel, M., Ng, C.W.W., 2018. Settlement and load transfer mechanism of a pile group adjacent to a deep excavation in soft clay. Comput. Geotech. 96, 55–72. https://doi.org/10.1016/j.compgeo.2017.10.010

Shen, Q., Liu, L., Yuan, J., 2017. Study on Design and Engineering Application of CFG Pile Composite Foundation. Bol. Téc. 55, 24–33.

Shen, Y., Wang, H., 2016. Optimization Design on CFG-Pile Foundation with Different Cushion Thickness in Beijing-Shanghai High-Speed Railway. Transp. Infrastruct. Geotechnol. 3, 3–20. https://doi.org/10.1007/s40515-015-0026-7

Shi, J., Wei, J., Ng, C.W.W., Lu, H., 2019. Stress transfer mechanisms and settlement of a floating pile due to adjacent multi-propped deep excavation in dry sand. Comput. Geotech. 116, 103216. https://doi.org/10.1016/j.compgeo.2019.103216

Soomro, M.A., Mangnejo, D.A., Bhanbhro, R., Memon, N.A., Memon, M.A., 2019. 3D finite element analysis of pile responses to adjacent excavation in soft clay: Effects of different excavation depths systems relative to a floating pile. Tunn. Undergr. Space Technol. 86, 138–155. https://doi.org/10.1016/j.tust.2019.01.012

Tan, S.A., Fellenius, B.H., 2016. Negative skin friction pile concepts with soil-structure interaction. Geotech. Res. 3, 137–147. https://doi.org/10.1680/jgere.16.00006

The professional standard of the People's Republic of China JGJ340-2015, 2015. Technical code for testing building foundation soils. China Building Industry Press, Beijing.

The professional standard of the People's Republic of China JGJ106-2014, 2014. Technical code for testing of building foundation piles. China Building Industry Press, Beijing.

Uba Uge, B., Guo, Y., 2020. Deep Foundation Pit Excavations Adjacent to Disconnected Piled Rafts: A Review on Risk Control Practice. Open J. Civ. Eng. 10, 270–300. https://doi.org/10.4236/ojce.2020.103023

Uge, B.U., Guo, Y.-C., 2020. CFG Pile Composite Foundation: Its Engineering Applications and Research Advances. J. Eng. 2020, 1–26. https://doi.org/10.1155/2020/5343472

Wang, G., Yang, Y., 2013. Effect of cantilever soldier pile foundation excavation closing to an existing composite foundation. J. Cent. South Univ. 20, 1384–1396. https://doi.org/10.1007/s11771-013-1626-4

Wei, Y., 2018. Research on evolutionary mechanisms and calculation method of earth pressure against rigid retaining walls close to rigid composite foundation (PhD Dissertation). Zhengzhou University, China.

Wu, C., Guo, W., Li, Y., 2016. Calculation of neutral surface depth and pile-soil stress ratio of rigid pile composite foundation considering influence of negative friction. Chin. J. Geotech. Eng. 38, 278–287. https://doi.org/10.11779/CJGE201602011

Zhang, D., Zhang, Y., Kim, C.W., Meng, Y., Garg, Akhil, Garg, Ankit, Fang, K., 2018. Effectiveness of CFG pile-slab structure on soft soil for supporting high-speed railway embankment. Soils Found. 58, 1458–1475. https://doi.org/10.1016/j.sandf.2018.08.007

Zhu, X., 2017. Analysis of the Load Sharing Behaviour and Cushion Failure Mode for a Disconnected Piled Raft. Adv. Mater. Sci. Eng. 2017, 1–13. https://doi.org/10.1155/2017/3856864